Nano Ferrite Incorporated Poly (Vinyl Pyrrolidone (PVP) /Poly (Vinyl Alcohol (PVA) Blend: Preparation and Investigation of Structural, Morphological and Optical Properties

Ali Jasim Mohammed[1*], Sameer H. Al-nesrawy[2]

Abstract

In this paper, the ferrite Cux Ni1-x FeO_3 when (x=0.1) has been prepared by the co-precipitation method and examined through the XRD-diffraction and confirming the face center cubic spinel phase (FCC) which attributed to the ferrite and found that these materials was Nano-scale. Then with different content of ferrite nanoparticle (1, 3 and 5 wt.%) additive to the (PVP/PVA) polymer matrix to synthesis (PVP/PVA/ferrite) nanocomposite by using casting method and study the Fourier transformation infrared (FTIR), (FE-SEM) and UV-Vis. Spectrophotometer. The FTIR confirming that there is no interactions between (PVP/PVA) polymer matrix and ferrite nanoparticles for all the sample prepared. From FE-SEM, the uniform morphology dispersed of ferrite inside the PVP/PVA blend with spherically shaped nanoparticles and the average grain size increased with increasing of concentration of ferrite. The absorption, absorption coefficient, transmittance and indirect energy band gap has been investigate.

Key Words: Ferrite, PVP, PVA, Optical Properties, Nanocomposite.

DOI Number: 10.14704/nq.2022.20.3.NQ22087 **NeuroQuantology 2022; 20(3):251-258**

Introduction

Nanocomposites are materials that, due to their high enactment, exhibit unexpected material pairings (Paul et al, 2008). Elastomers and engineering plastics are in high demand, and their capabilities are so impressive that they use in different application, from packaging to various applications (Jappor, 2016; Abbas et al, 2017; Moniruzzaman et al, 2006). Nano-composites polymers, which consist of organic polymers and inorganic nanoparticles in a nanoscale area, are unique kinds of properties that received a lot of attention at last year's conference. (Abdelamir et al, 2020; Al-Rubaye et al, 2020; Winey et al, 2007). Some of unique properties of these composite are different from those of pure polymers (Bhaiswar et al, 2014; Jawadet al 2011; Li et al, 2010).

Corresponding author: Ali Jasim Mohammed

Address: [1*]Department of Physics, Faculty of Education for Pure Science, University of Babylon, Iraq; [2]Department of Physics, Faculty of Education for Pure Science, University of Babylon, Iraq.

[1*]E-mail: a.alijasim.aj@gmail.com

Relevant conflicts of interest/financial disclosures: The authors declare that the research was conducted in the absence of any commercial or financial relationships that could be construed as a potential conflict of interest.

Received: 11 January 2022 **Accepted:** 17 February 2022

Ferrites are ceramic materials that appear dark grey or black and are extremely hard and brittle. Ferrites classified as magnetic materials due to their ferromagnetic behavior and used in the different application (Thurn et al, 2000; Li et al, 2003; Kennedy et al, 2012; Williams et al, 2018). Thermal, co-precipitation, solution combustion using various types of organic fuels, sol–gel approaches, hydrothermal and electrochemical techniques (Aisida et al 2019; Al-Nesraway et al, 2018; Zhu et al, 2014; Iqbal et al, 2016; Hu et al, 2008 – Elsayed et al, 2016) can all be used to produce ferrites in powder or thin film form.

Because of its excellent transparency and good ecological stability, poly (vinyl pyrrolidone (PVP) has piqued the interest of researchers. PVP has unique electrical, optical and mechanical properties, therefore used in different application (Wöhrle, 2005; Sreekanth et al, 2019; Fischer et al, 2009). Polyvinyl alcohol (PVA) is a polymer with numerous unique physical properties that are used in practical applications. PVA is a semi-crystalline, water-soluble, low electrical conductivity material with excellent film forming and adhesive properties that can be used in different applications (Zhai et al, 2008).

In the study, PVP/PVA/ferrite nanocomposite with the different weight concentration of ferrite nanoparticle has been manufactured by in co-precipitation technique and study the effect additive of the ferrite nanoparticle on the structural (XRD, FTIR), morphological (SEM) and optical properties.

Experimental

1. Materials and Methods

Ferric chloride $FeCl_3$ was manufactured in Spain, RBL Sr.No.9066 with a purity of 99.9 percent, copper nitrate $Cu(NO_3)_2.3H_2O$ with a purity of 98 percent was purchased in Spain, Barcelona, and nickel nitrate Ni $(No_3)_2.6H_2O$ In Korea, Gyeonggi-do, with 98 percent purity was purchased. Hi Media, India, supplied PVP and PVA with average molecular weights of 40,000 and 18000, respectively. The solvent for the a whole fabrication was deionized water.

Synthesis of the Ferrite Nanoparticle

$Cu_xNi_{1-x}FeO_3(x=0.1)$ were synthesized by co-precipitation method. Usually, 2.416 gm copper nitrate, 26.172gm nickel nitrate and 1.622 gm ferric chloride were mixed thoroughly with 100 ml of deionized water solution. This combination was then heated to 50°C for 1hr and then add NaOH solution until the PH value in the solution is greater or equal to 7 with stirring, filter the solution and then wash it with distilled water. Drying at 150°C, Grinding and lastly Calcined at 1200°C for 6 hours.

Synthesis of the (PVP/PVA/ferrite) Nanocomposites

(PVP/PVA/ferrite) nanocomposites have been prepared which mixed (70 wt. %) of PVP and (30 wt%) of PVA in (50) ml of deionized water with magnetic stirrer to get additional homogenous solution. Ferrite nanoparticles were added to solution with varying percentage (1, 3 and 5) wt% and using casting method to fabricate (PVP/PVA/ferrite) nanocomposites. Using the XRD-Diffraction, FTIR, FE-SEM and optical properties to investigate nanocomposite prepared.

Result and Discussion

The X-ray diffraction of the ferrite nanoparticle are shown in fig. (1). From this figure, shows the peaks at 2θ (30.36, 35.73°, 37.19°, 43.22°, 57.53°, 63.34°, 75.81° and 79.24°) identical to the card (JCPDS 00-047-1049) (Mirzaee et al,2018)confirming the face center cubic spinel phase (FCC) and all samples prepared without the presence of impurities or secondary phases and this proves that the method of preparation includes the incorporation of positive ions into the spinel structure (Mallesh et al, 2019). The average crystallite size have been calculated from the Scherer's equation (Abud et al, 2012):

$$D = \frac{0.9\lambda}{\beta\cos\theta\beta} \qquad (1)$$

Where (λ) Wavelength of incident X-ray radiation (1.54056Å), (β): Full width at half maximum of the peak (radian). (θ)β Bragg diffraction angle of the XRD peak (degree).

The average crystallite size was 26.08 nm. The d-spacing are listed in Table (1). This result is agreement with the previous studies (Gao at el, 2018; Rashidi at el, 2016).

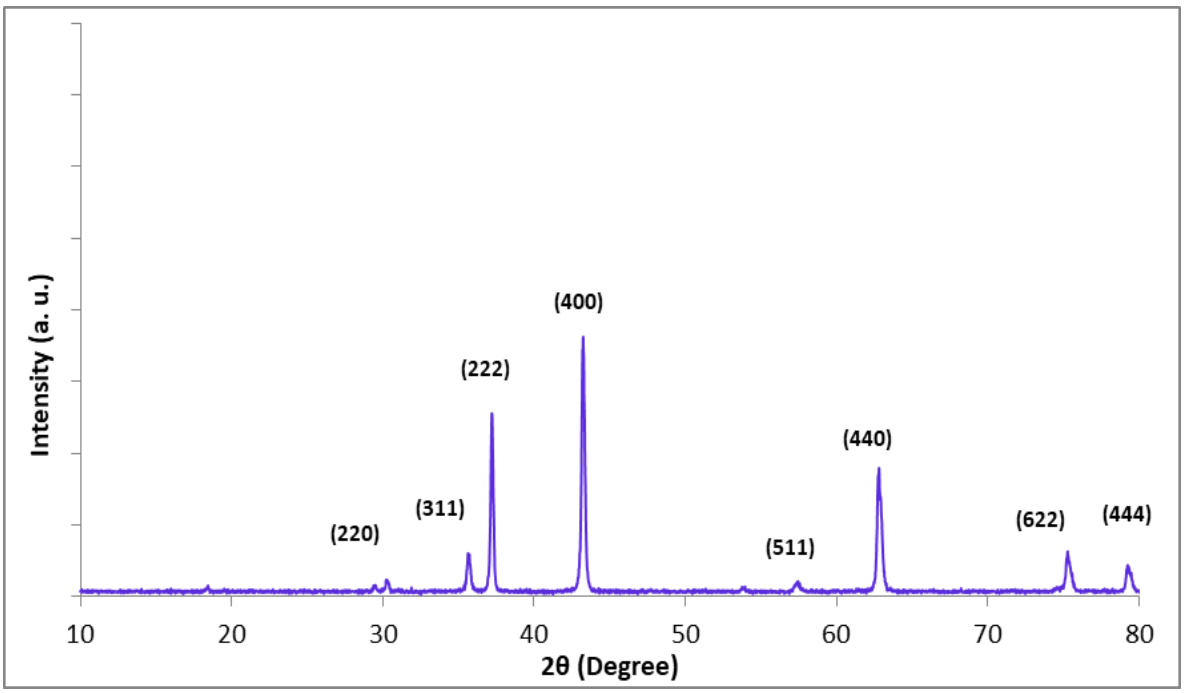

Fig. 1. The XRD pattern of the ferrite nanoparticle

Table 1. The obtained result of the XRD for the ferrite nanoparticle

Component	2θ (degree)	(hkl)	FWHM (degree)	d(Å)	Crystallite size (nm)	Average Crystallite size (nm)
Ferrite	30.36	(220)	0.37	2.940	22.25	26.08
	35.73	(311)	0.478	2.510	17.46	
	37.19	(222)	0.299	2.415	27.95	
	43.22	(400)	0.434	2.091	19.66	
	57.53	(511)	0.41	1.600	22.10	
	63.34	(440)	0.24	1.467	38.89	
	75.81	(622)	0.28	1.253	35.95	
	79.24	(444)	0.423	1.207	24.36	

FE-SEM of the (PVP/PVA/ferrite) nanocomposite with various content of the ferrite are revealed in fig.(2). In this figure, the symbol A, B,C and D indicate to pure PVP/PVA, PVP/PVA/(1%wt.) ferrite, PVP/PVA/(3% wt.) ferrite and PVP/PVA/ (5%wt.) ferrite respectively. From this figure, it is observed that the pure PVP/PVA was homogenous and smooth this indicate a good method for prepared films. Also the uniform morphology dispersed of ferrite inside the PVP/PVA blend with spherically shaped nanoparticles. The homogeneous nanoparticles dispersed in the polymeric matrix is owing to the strong interfacial interface between of nanoparticles and the blend components. The Table (2) was obtained that the average particle size increased with increasing of concentration of ferrite, it is increased from 32.37 nm for A_1 to 44.83 nm for A_3. This result are agreement with previous studied (Ramesan et al, 2018; Carvalho et al, 2018; Abid et al, 2021).

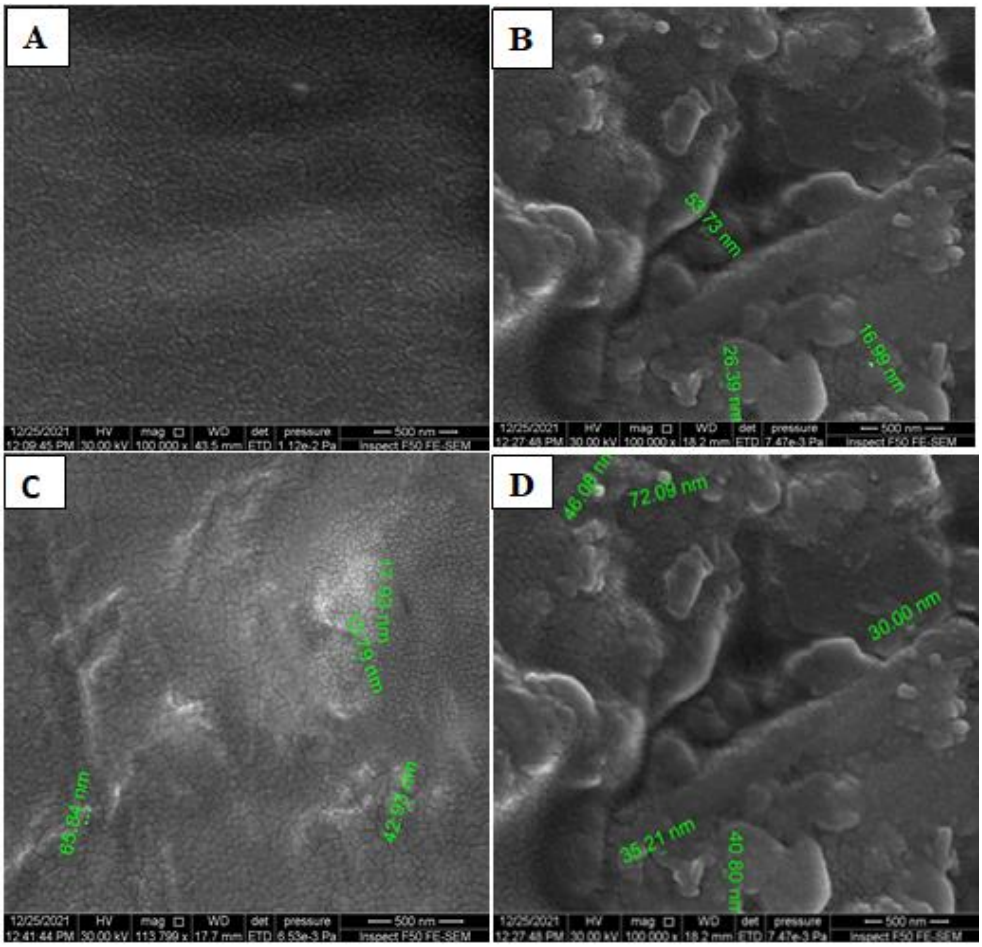

Fig. 2. FE-SEM images for all the sample prepared of nanocomposite with different concentration

Table 2. The average grain size for all the sample prepared

Sample	Average grain size (nm)
A	0
B	32.37
C	35.12
D	44.83

FTIR spectra of (PVP/PVA/ferrite) nanocomposites with different concentration (1, 3, and 5 wt.%) of ferrite are revealed in fig.(3). In this figure, the symbol A, B,C and D indicate to pure PVP/PVA, PVP/PVA/(1%wt.) ferrite, PVP/PVA/(3% wt.) ferrite and PVP/PVA/(5%wt.) ferrite respectively. The existence of OH groups in the polymer matrix chain results in the appearance of a wide band at 3365 cm^{-1} for all specimens produced of nanocomposites. The band at 2922 cm^{-1} is indicative of an asymmetry stretching mode of the CH_2 group. The C-H groups were responsible for the band at (2360) cm^{-1}. There are four strong peaks observed for all the sample of nanocomposite at (1648, 1422 and 1288,1092) cm^{-1} belong to C=O groups, C-O groups, CH_2 bending and C-O bonds of polymers matrix respectively. Changes in the spectral of (PVP/PVA) caused by ferrite nanoparticles include a shift in some bonds and a variation in intensities. The interactions of nanoparticles with polymers were responsible for these changes. FTIR analysis reveals no interactions between the (PVP/PVA) blend and the ferrite nanoparticles. The transmission reduce slightly as the concentration of ferrite nanoparticles increases, which is due to an increase in nanocomposite density. These findings are supported by the researchers. (Ali et al, 2020; Toman et al, 2021).

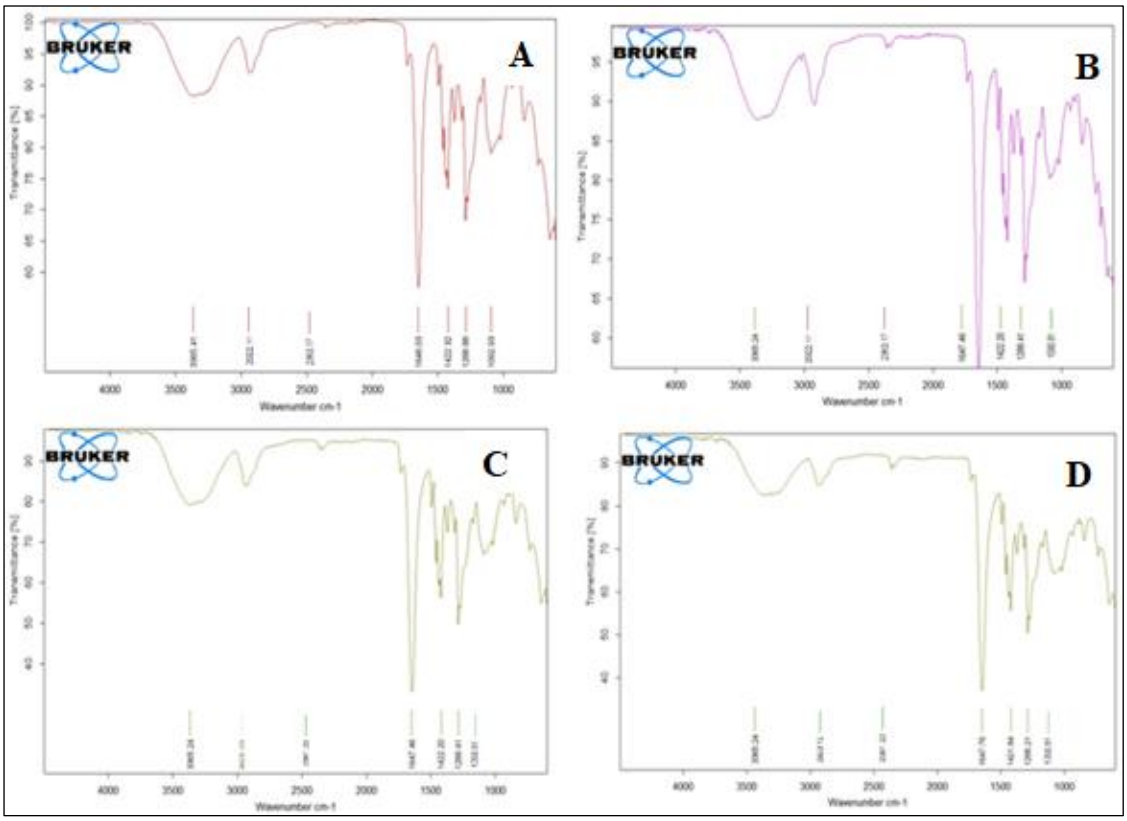

Fig. 3. FTIR spectrum for all the sample prepared of nanocomposite with different concentration ferrite

The absorption of (PVP-PVA/ferrite) nanocomposite with different concentrations of ferrite has been recorded at wavelengths range (220-820) nm at room temperatures. Fig.(4) show the absorbance spectra for all the sample prepared. It is observe that the absorption rise when the additive ferrite nanoparticle which is due to donor level electron excitations to the conduction band at these energies and reduce the transmittance are shown in fig. (5) (Indolia et al, 2013; Abass et al, 2019; Feng et al, 2015; Abid et al, 2021).

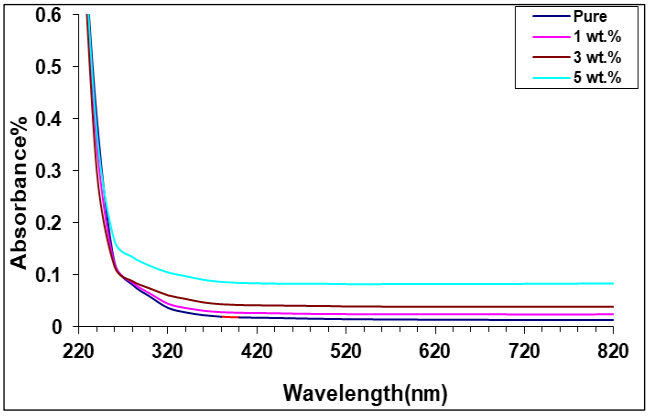

Fig. 4. The absorbance as a function of wavelength of (PVP/PVA/ferrite) nanocomposites with different concentrations

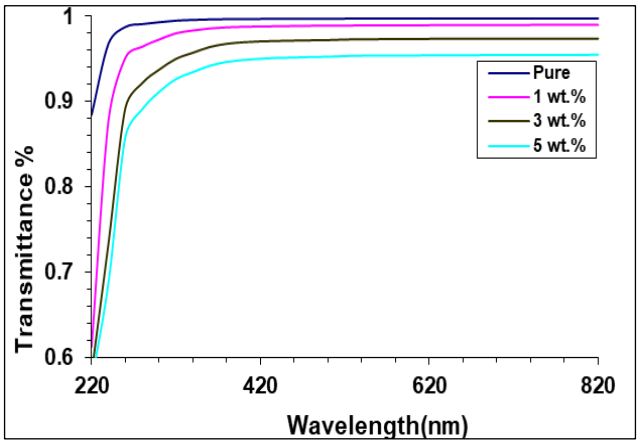

Fig. 5. The transmittance variation of (PVP/PVA/ferrite) nanocomposites with the wavelengths

The absorption coefficient of nanocomposite can be calculate by the relation (Marien et al, 2000):

$$\alpha = 2.303A/t \qquad (2)$$

Where (A) absorption and (α) absorption coefficient.

The absorption coefficient used to know the nature of the transition. Fig.(6) reveals to the absorption coefficient of the (PVP-PVA/ferrite) nanocomposite. The $\alpha < 10^4$ cm^{-1} which indicate to the indirect

transition (Khadayeir et al, 2018; Salman et al, 2015).

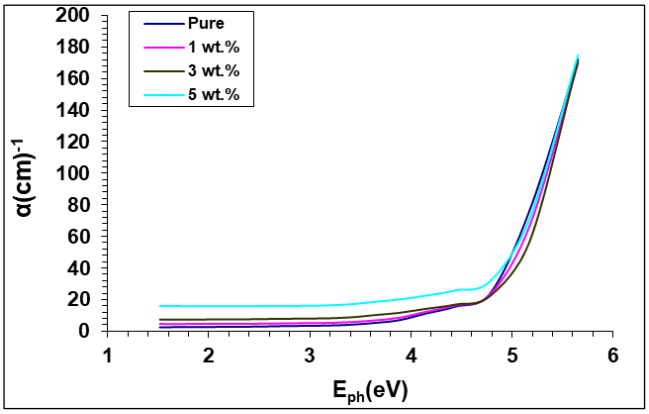

Fig. 6. The absorption coefficient variation of nanocomposites with the photon energies

The energy band gap of (PVP/PVA/ferrite) nanocomposite has been calculated from the following equation (Abdelghany et al, 2014):

$$\alpha h\upsilon \approx B(h\upsilon - Eg)^r \quad (3)$$

Where B is a constant, hυ is the energy of photons, E_g is the band gap optical energy and r = 2 for allowed indirect transitions and r = 3 for forbidden-indirect transitions.

Fig. (7,8) show the energies gap for the (PVP-PVA/ferrite) nanocomposite. According to these figures, the E_g rise when the increase of the ferrite content due to the formation of levels in the energy gap which lead to reduce energy gap. The value of these energies are listed in Table (3).

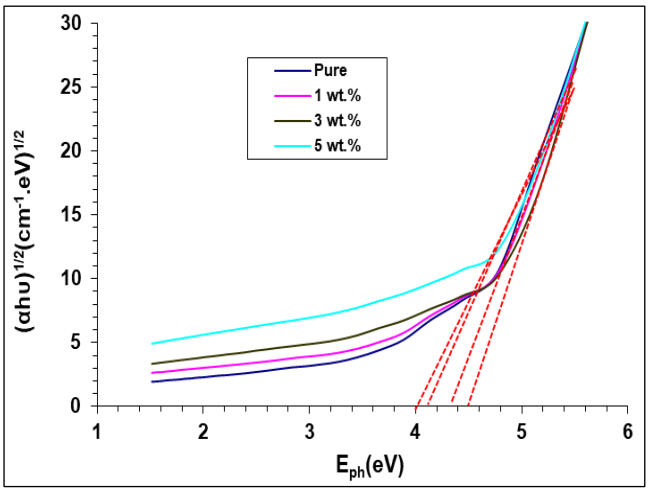

Fig. 7. The energy gap for the allowed indirect transition $(\alpha h\nu)^{1/2}$ $(cm^{-1}.eV)^{1/2}$ versus photon energy of (PVP/PVA/ferrite) nanocomposite with different concentration

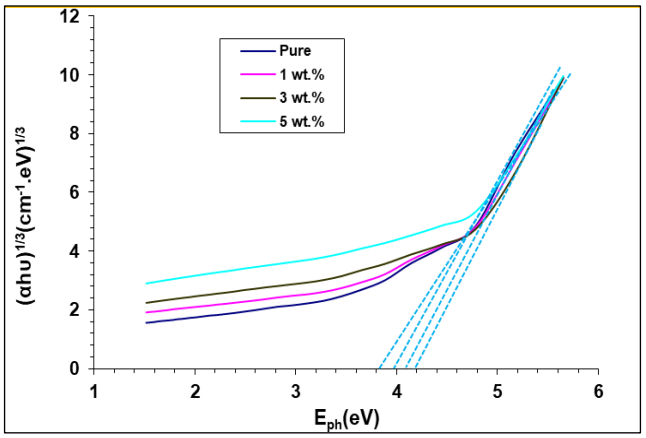

Fig. 8. The Energy gap for the forbidden indirect transition $(\alpha h\nu)^{1/3}$ $(cm^{-1}.eV)^{1/3}$ versus Photon energy of the (PVP/PVA/ ferrite) nanocomposite with different concentration

Table 3. The values of optical energy gap for allowed indirect transitions of (PVP/PVA/ferrite)

Wt% Ferrite	Allowed indirect transition	Forbidden indirect transition
0	4.5	4.2
1	4.3	4.1
3	4.1	4
5	4	3.82

256

Conclusion

In summary, this study found:

1. The spinel ferrite were successfully synthesized by co-precipitation method and examined by the XRD-diffraction and found that these materials was Nano-scale where average crystalline size was 26.08 nm.
2. FTIR of the (PVP/PVA/ferrite) confirm that there is no interaction between the ferrite and polymer blend which mean happen composite.
3. FE-SEM found the uniform morphology homogenies distribution of the ferrite inside the polymer blend and found that the grain size increased with increasing concentration of ferrite.
4. The absorbance and the absorption coefficient increase with increasing concentration of the ferrite nanoparticle and the transmission and energy band gap decreased with rise content of the ferrite nanoparticle.

References

Abbas, M.M., & Abdulridha, A.R. (2017). Influences of Heat Treatment on Superconducting Properties of Bi1. 7Pb0. 3 (nanoTi0.2) $Sr_2Ca_2Cu_3O10+d$ Thin Film Deposited on Different Substrates. *Energy Procedia,* 119, 367-375.

Abdelghany, A.M., Abdelrazek, E.M., & Rashad, D.S. (2014). Impact of in situ preparation of CdS filled PVP nano-composite. *Spectrochimica Acta Part A: Molecular and Biomolecular Spectroscopy,* 130, 302-308.

Abdelamir, A.I., Al-Bermany, E., & Hashim, F.S. (2020). Important factors affecting the microstructure and mechanical properties of PEG/GO-based nanographene composites fabricated applying assembly-acoustic method. *In AIP Conference Proceedings,* 2213(1).

Abid, A.A., Al-nesrawy, S.H., & Abdulridha, A.R. (2021). New Fabrication (PVA-PVP-C. B) Nanocomposites: Structural and Electrical Properties. *In Journal of Physics: Conference Seri*es 1804(1).

Abid, A.A., Al-nesrawy, S.H., & Abdulridha, A.R. (2021). New Fabrication (PVA-PVP-C. B) Nanocomposites: Structural and Electrical Properties. *In Journal of Physics: Conference Series* 1804(1).

Aisida, S.O., Akpa, P.A., Ahmad, I., Maaza, M., & Ezema, F.I. (2019). Influence of PVA, PVP and PEG doping on the optical, structural, morphological and magnetic properties of zinc ferrite nanoparticles produced by thermal method. *Physica B: Condensed Matter,* 571, 130-136.

Abud, S.H., Hassan, Z., & Yam, F.K. (2012). Enhancement of structural and optical properties of porous In0.27Ga0.73N thin film synthesized using electrochemical etching technique. *Int. J. Electrochem. Sci,* 7, 10038-10046.

Abass, K.H., & Mohammed, M.K. (2019). Fabrication of ZnO: Al/Si solar cell and enhancement its efficiency via Al-doping. *Nano Biomed. Eng,* 11(2), 170-177.

Al-Nesraway, S.H., Al-Maamori, M.H., & Al-Issawe, J.M. (2018). Preparation of a rubber nanocomposite (Silicone Rubber-Ferrite) for protect human from bioeffects of microwave emitted from mobile devices. *Journal of Bionanoscience,* 12(5), 645-651.

Al-Rubaye, S., Al-bermany, E., Habeeb, M., & Rajagopalan, R. (2020). Electrochemical Performance Evaluation of Ni foam/NiCo2O4-CNTs for Energy Storage Applications. pdf. *Test Engineereing and Management,* 83, 12828-41.

Ali, R.S., Mohammed, M.K., Khadayeir, A.A., Abood, Z.M., Habubi, N.F., & Chiad, S.S. (2020). Structural and Optical Characterization of Sprayed nanostructured Indium Doped Fe_2O_3 Thin Films. *In Journal of Physics: Conference Series* (Vol. 1664, No. 1, p. 012016). IOP Publishing.

Bhaiswar, J.B., Salunkhe, M.Y., Dongre, S.P., & Kumbhare, B.T. (2014). Comparative study on thermal stability and optical properties of PANI/CdS and PANI/PbS nanocomposite. *IOSR J. Appl. Phys.(ICAET-2014),* 80, 79-82

Carvalho, A.J.F., Trovatti, E., & Casale, C.A. (2018). Polystyrene/cellulose nanofibril composites: fiber dispersion driven by nanoemulsion flocculation. *Journal of Molecular Liquids,* 272, 387-394.

Elsayed, E.M., Rashad, M.M., Khalil, H.F.Y., Ibrahim, I. A., Hussein, M.R., & El-Sabbah, M.M.B. (2016). The effect of solution pH on the electrochemical performance of nanocrystalline metal ferrites MFe_2O_4 (M= Cu, Zn, and Ni) thin films. *Applied Nanoscience,* 6(4), 485-494

Feng, Y., Dong, N., Wang, G., Li, Y., Zhang, S., Wang, K., & Wang, J. (2015). Saturable absorption behavior of free-standing graphene polymer composite films over broad wavelength and time ranges. *Optics Express,* 23(1), 559-569.

Fischer, F., & Bauer, S. (2009). Polyvinylpyrrolidon (PVP): ein vielseitiges Spezialpolymer — Verwendung in der Keramik und als Metallabschreckmedium. *Keramische Zeitschrift,* 61(6), 382-385.

Gao, Y., Wang, Z., Pei, J., & Zhang, H. (2018). Structure and magnetic properties correlated with cation distribution of Ni0. 5-xMoxZn0. $5Fe_2O_4$ ferrites prepared by sol-gel auto-combustion method. *Ceramics International,* 44(16), 20148-20153.

Hu, C., Gao, Z., & Yang, X. (2008). One-pot low temperature synthesis of MFe_2O_4 (M= Co, Ni, Zn) superparamagnetic nanocrystals. *Journal of Magnetism and Magnetic Materials,* 320(8), L70-L73.

Indolia, A.P., & Gaur, M.S. (2013). Optical properties of solution grown PVDF-ZnO nanocomposite thin films. *Journal of Polymer Research,* 20(1), 1-8.

Iqbal, F., Abd Mutalib, M.I., Shaharun, M.S., & Abdullah, B. (2016). Synthesis of $ZnFe_2O_4$ using sol-gel method: effect of different calcination parameters. *Procedia engineering,* 148, 787-794.

JAPPOR, H.R. (2016). Effect of temperature on rheological properties of sbr compounds reinforced by some industrial scraps as a filler. *Int. J. Chem. Sci.,* 14, 1285-1295.

Jawad, E., Khudhair, S.H., & Ali, H.N. (2011). A thermodynamic study of adsorption of some days on Iraqi Bentoniet modified clay. *European Journal of Scientific Research,* 60(1), 63-70

Khadayeir, A.A., Abass, K.H., Chiad, S.S., Mohammed, M.K., Habubi, N.F., Hameed, T.K., & Al-Baidhany, I.A. (2018). Study the influence of Antimony Trioxide (Sb2O3) on optical properties of (PVA-PVP) composite. *Journal of Engineering and Applied Sciences*, 13(22), 9689-9692.

Kennedy, J., Leveneur, J., Takeda, Y., Williams, G.V.M., Kupke, S., Mitchell, D.R.G., & Metson, J.B. (2012). Evolution of the structure and magneto-optical properties of ion beam synthesized iron nanoclusters. *Journal of Materials Science,* 47(3), 1127-1134.

Li, S., Meng Lin, M., Toprak, M.S., Kim, D.K., & Muhammed, M. (2010). Nanocomposites of polymer and inorganic nanoparticles for optical and magnetic applications. *Nano reviews,* 1(1), 5214.

Li, D., Herricks, T., & Xia, Y. (2003). Magnetic nanofibers of nickel ferrite prepared by electrospinning. *Applied physics letters,* 83(22), 4586-4588.

Moniruzzaman, M., & Winey, K.I. (2006). Polymer nanocomposites containing carbon nanotubes. *Macromolecules,* 39(16), 5194-5205.

Mirzaee, S., & Shayesteh, S.F. (2018). Ultrasound induced strain in ultrasmall $CoFe_2O_4$@ polyvinyl alcohol nanocomposites. *Ultrasonics Sonochemistry,* 40, 583-586.

Mallesh, S., & Srinivas, V. (2019). A comprehensive study on thermal stability and magnetic properties of MnZn-ferrite nanoparticles. *Journal of Magnetism and Magnetic Materials,* 475, 290-303.

Marien, J., Wagner, T., Duscher, G., Koch, A., & Rühle, M. (2000). Nb on (110) TiO2 (rutile): growth, structure, and chemical composition of the interface. *Surface science,* 446(3), 219-228.

Mohammed, M.K., Al-Dahash, G., & Al-Nafiey, A. (2020). Synthesis and characterization of PVA-Graphene-Ag nanocomposite by using laser ablation technique. *In Journal of Physics: Conference Series,* 1591(1).

Paul, D.R., & Robeson, L.M. (2008). Polymer nanotechnology: nanocomposites. *Polymer,* 49(15), 3187-3204.

Philippova, O., Barabanova, A., Molchanov, V., & Khokhlov, A. (2011). Magnetic polymer beads: Recent trends and developments in synthetic design and applications. *European polymer journal,* 47(4), 542-559.

Ramesan, M.T., Anjitha, T., Parvathi, K., Anilkumar, T., & Mathew, G. (2018). Nano zinc ferrite filler incorporated polyindole/poly (vinyl alcohol) blend: Preparation, characterization, and investigation of electrical properties. *Advances in Polymer Technology,* 37(8), 3639-3649.

Rashidi, S., & Ataie, A. (2016). Structural and magnetic characteristics of PVA/CoFe2O4 nano-composites prepared via mechanical alloying method. *Materials Research Bulletin,* 80, 321-328.

Salman, S.A., Bakr, N.A., & Mahmood, M.H. (2015). Preparation and Study of Some Electrical Properties of PVA-Ni (NO 3) 2 Composites. *International Letters of Chemistry, Physics and Astronomy,* 40.

Sreekanth, K., Siddaiah, T., Gopal, N.O., Krishna Jyothi, N., Vijaya Kumar, K., & Ramu, C. (2019). Optical and conductivity studies of Cr3+ doped polyvinyl pyrrolidone polymer electrolytes. *Journal of Macromolecular Science, Part B,* 58(11), 860-876.

Thurn-Albrecht, T., Schotter, J., Kastle, G.A., Emley, N., Shibauchi, T., Krusin-Elbaum, L. & Russell, T.P. (2000). Ultrahigh-density nanowire arrays grown in self-assembled diblock copolymer templates. *Science,* 290(5499), 2126-2129.

Toman, M. S., & Al-nesrawy, S. H. (2021). New Fabrication (PVA-CMC-PbO) Nanocomposites Structural and Electrical Properties. NeuroQuantology, 19(4), 38.

Williams, G.V., Prakash, T., Kennedy, J., Chong, S.V., & Rubanov, S. (2018). Spin-dependent tunnelling in magnetite nanoparticles. *Journal of Magnetism and Magnetic Materials,* 460, 229-233.

Winey, K.I., & Vaia, R.A. (2007). Polymer nanocomposites. *MRS bulletin,* 32(4), 314-322

Wöhrle, D. (2005). Macromolecular metal complexes: materials for various applications. Angewandte Chemie International Edition, 44(46), 7500-7502..

Zhai, L.L., Ling, G.P., & Wang, Y.W. (2008). Effect of nano-Al2O3 on adhesion strength of epoxy adhesive and steel. *International journal of adhesion and adhesives,* 28(1-2), 23-28.

Zhu, X., Zhang, F., Wang, M., Ding, J., Sun, S., Bao, J., & Gao, C. (2014). Facile synthesis, structure and visible light photocatalytic activity of recyclable $ZnFe_2O_4/TiO_2$. *Applied surface science*, 319, 83-89.